Available online at www.sciencedirect.com
SCIENCE DIRECT
Polymer 46 (2005) 8752–8762
polymer
www.elsevier.com/locate/polymer

Sequence distribution, crystallization and melting behavior of poly(ethylene terephthalate-*co*-trimethylene terephthalate) copolyesters

Chi-Yun Ko[a], Ming Chen[a,*], Hui-Chen Wang[a], I-Min Tseng[b]

[a]*Institute of Materials Science and Engineering, National Sun Yat-Sen University, Kaohsiung 80424, Taiwan, ROC*
[b]*Union Chemical Laboratories, Industrial Technology Research Institute, Hsinchu 300, Taiwan, ROC*

Received 16 October 2004; received in revised form 21 January 2005; accepted 25 January 2005
Available online 27 June 2005

Abstract

The compositions of a series of copolyesters of ethylene- and trimethylene- terephthalate were determined by NMR. The values of randomness parameter revealed these copolyesters were random copolymers with average-number sequence lengths varied from 1 to 10. These copolyesters were investigated using temperature-modulated differential scanning calorimeter (TMDSC) and wide angle X-ray diffractometer (WAXD). The crystallization behavior was evidenced from the non-isothermal DSC thermograms and WAXD patterns. The crystallization rate and the intensity of diffraction peaks decrease with increasing the minor co-monomer content. The copolyester with equal amounts of monomers is still crystallizable even though the average sequence length is only 2.0, and its WAXD pattern is quite different from those of homopolymers. In the melting study, three distinct peaks of reversing melting were observed. Two peaks in the high temperature side are due to remelting of the recrystallized crystals formed during the heating scan, whereas the highest temperature peak is attributed to the melting of the crystals that are formed in relatively high temperature. The results of WAXD and TMDSC support the mechanism of melting-recrystallization-remelting for the multiple melting behaviors.

Keywords: Copolyester; TMDSC; WAXD

1. Introduction

Linearly polymerized esters of terephthalic acid and glycols have been synthesized by Whinfield and Dickson in 1941, and have been patented in 1946 and 1949 [1,2]. It is advantageous to use glycols having from 2 to 4 methylene groups, since these give highly polymerized esters with very high melting points. Poly(ethylene terephthalate) (PET) has the melting point of 265 °C, whereas the melting points of poly(trimethylene terephthalate) (PTT) and poly(butylene terephthalate) (PBT) are nearly identical (233 and 232 °C, respectively) [3]. For a long time, PTT did not find commercial interest due to the limited availability of 1,3-propanediol (3G), the monomer used for PTT synthesis. Recently, PTT has drawn attention because of Shell's breakthrough in lower-cost monomer processes [4].

PET is a slow crystallizing material [5,6]. PTT can be crystallized easily without adding nucleation agents [7,8]. Modifications of the chemical composition and the sequence distribution of semicrystalline polymers by copolymerization will alter both the crystallization kinetics and the morphology. Up to now, the synthesis and characterization of poly(ethylene terephthalate-*co*-trimethylene terephthalate) (PET/PTT) copolyesters were reported in a few articles [9–14]. Most of these copolyesters were crystallizable, but some were amorphous depending on the compositions [9–11,13,14]. In 1966, Smith et al. [9] presented the accumulated data on polyesters and copolyesters of the poly(methylene terephthalate) series that they have studied. It was expected and found that a eutectic composition existed having a minimum melting point for the copolyesters. Under the conditions employed in the measuring technique of differential thermal analysis (DTA), no DTA melting points (T_m) are recorded for the PET/PTT copolyesters containing 40–50 mol% of 3G. However, their melting points can be found using a Fisher-Johns melting point apparatus. Ponnusamy and Balakrishnan [10,11] synthesized a series of random copolyesters from dimethyl

* Corresponding author. Tel.: +886 7 382 4680; fax: +886 7 525 4099.
E-mail address: mingchen@mail.nsysu.edu.tw (M. Chen).

0032-3861/$ - see front matter © 2005 Elsevier Ltd. All rights reserved.
doi:10.1016/j.polymer.2005.01.107

terephthalate (DMT), ethylene glycol (2G) and 3G by melt polycondensation techniques. However, the obtained PET/PTT copolyesters had a low molecular weight with the intrinsic viscosity ranging from 0.09 to 0.18 dl/g (solvent: *o*-chlorophenol, 30±0.1 °C). The number average molecular weights determined from vapor pressure osmometer were between 1500 and 3050 g/mol. As the 3G content increases, the copolyester becomes more amorphous and there is no melting temperature for the copolyesters with 71.0 and 77.7 mol% of 3G. When the composition of 3G reaches 100 mol%, the copolymer becomes crystalline again. Recently, a series of PET/PTT copolyesters was synthesized by reacting DMT, 2G, and 3G in a two-step reaction sequence [13]. The composition was determined by proton nuclear magnetic resonance (^{1}H NMR). Their thermal properties and non-isothermal crystallization kinetics were studied by differential scanning calorimetry (DSC). It was found that the copolymers containing 32.8 mol%≤3G≤39.3 mol% were amorphous, whereas the copolymers with 46, 58 and 78 mol% of 3G were crystallizable. Wu and Lin [14] mentioned that the amorphous copolymers contained 34–56 mol% of 3G which covers both ranges of 33–39 mol% [13] and 40–50 mol% [9] of 3G.

In this study, ^{13}C NMR was used to determine the composition and the sequence distribution of the PET/PTT copolyesters. Their intrinsic viscosities were measured in a mixed solvent. The co-crystallization of a series of copolyesters was evidenced from the non-isothermal DSC thermograms and the wide-angle X-ray diffractograms (WAXD). In addition, the origin of multiple melting behaviors of non-isothermal crystallized specimens was elucidated by WAXD and temperature modulated differential scanning calorimetry (TMDSC).

2. Experimental

2.1. Materials and characterization

Developmental grade PET/PTT copolyesters were prepared by two steps. The first step was the esterification reaction of terephthalic acid (TPA) and 3G at 245 °C for 3.5 h under nitrogen. Oligomer of bis(3-hydroxypropyl) terephthalate (BHPT) was produced at a calculated esterification conversion of 98.1%. In the second step, BHPT, TPA, and 2G were reacted together in an esterification reaction of the same condition. Then, the esterified product was subjected to undergo a polycondensation reaction at 255 °C for 4 h under a vacuum of less than 1 Torr.

The sample codes, the feed composition of 3G and 2G are tabulated in the first three columns of Table 1. The intrinsic viscosity [η] of these aromatic polyesters was measured in a mixed solvent of phenol/1,1,2,2-tetrachloroethane (3/2, w/w) at 25±0.2 °C using an Ubbelohde viscometer. Their values, ranged from 0.62 to 0.84 dl/g, are listed in the fourth column. Gel Permeation Chromatography (GPC) was performed at 120 °C on a Waters 150CV GPC. HPLC grade *m*-Cresol was used as the mobile phase at a flow rate of 1.0 ml/min with two Waters high temperature (HT) Styragel columns in series. The number average molecular weights, $\bar{M}_n$, and the weight average molecular weights, $\bar{M}_w$, of PT62/ET38, PT50/ET50, PT22/ET78 and PT09/ET91 samples are $(2.6\pm0.2)\times10^4$ and $(6.6\pm0.6)\times10^4$ daltons/mole, respectively, as shown in the last two columns of Table 1. Their polydispersity values are 2.5±0.1.

The copolyester pellets were sandwiched between two polyimide films and two copper plates, and then they were put in a hot press machine. The compressed film had a thickness of about 0.2 mm. Both pellets and films were dried at 45 °C in a vacuum oven for 12 h before using. Amorphous specimens, quenched from the melt, were prepared for the experiments of non-isothermal crystallization.

2.2. Composition and sequence analysis

The ^{13}C NMR and ^{1}H NMR spectra of $CDCl_3/CF_3COOD$ (1/4, v/v) solutions were recorded on the Bruker AMX-400 NMR spectrometer at 320 K. To perform quantitative ^{13}C NMR measurement, one should take into account the difference of spin-lattice relaxation time (T_1) among various carbons. The values of T_1 were located between 0.16 and 3.7 s, as shown in Fig. 1. In order to have a quantitative response, the ^{13}C NMR spectra were determined by using a 20-s pulse cycle. This condition ensured the complete relaxation of all the analyzed nuclei, therefore, the relative peak areas could be measured in an automatic integration mode.

2.3. Non-isothermal crystallization

Non-isothermal crystallization from the amorphous states of glass and melt was conducted on a TMDSC (TA model Q100), equipped with a refrigerated cooling system. Nitrogen gas was used as the purge gas with a flow rate of 50 ml/min. The weight of these samples was between 2 and 3 mg. Both temperature and heat flow were calibrated by indium standard. In the conventional mode of TMDSC, each amorphous sample was heated at a rate of 5 °C/min from 25 to 285 °C, and then held for 3 min to remove thermal history. Subsequently, each sample was cooled to 30 °C at 5 °C/min.

2.4. Wide angle X-ray diffraction

Melt-crystallized copolyesters were crystallized completely at a temperature of 30–40 °C below their equilibrium melting temperatures (T_m^0), as shown in the second column of Table 4. X-ray diffractograms at room temperature were acquired by a Siemens D5000 diffractometer using

Table 1
Sample code, feed composition, intrinsic viscosity and the relative number-average, weight-average molecular weights of aromatic polyesters

Sample code	Feed composition (mol%)		[η] (dl/g)	M_n (10^{-4})	M_w (10^{-4})
	3G	2G			
PTT	100	0	0.83	N/A	N/A
PT91/ET09	80	20	0.84	N/A	N/A
PT71/ET29	60	40	0.70	N/A	N/A
PT62/ET38	50	50	0.70	2.8	7.2
PT50/ET50	40	60	0.70	2.7	6.6
PT27/ET73	20	80	0.66	N/A	N/A
PT22/ET78	15	85	0.64	2.7	7.0
PT09/ET91	5	95	0.62	2.4	5.7
PET	0	100	0.70	N/A	N/A

N/A: not available.

Ni-filtered Cu K_α radiation ($\lambda = 0.1542$ nm, 40 kV, 30 mA) at a scanning rate of 1°/min. The other sets of the X-ray diffractograms were obtained in the same way for each PET/PTT copolyester isothermally crystallized at various temperatures.

2.5. Melting behavior after non-isothermal cooling

Melting behavior was also investigated on a TA Instruments Q100. The condition and the calibration are described in the previous section. In addition, a standard sapphire sample was used to measure the heat capacity calibration constant. Each sample was heated at a rate of 20 °C/min to a pre-melting temperature above its T_m^0 (see columns 3 and 2 of Table 4), and then held at that temperature for 5 min to remove the thermal history. Subsequently, each sample was cooled to 30 °C at a rate of 5 °C/min. In the modulated mode of TMDSC, non-isothermal crystallized specimens were heated at a rate of 3 °C/min with an oscillation amplitude of 0.318 °C and period of 40 s, based upon the recommended specifications given in the instrument manual [15]. The PT91/ET09 specimen was conducted at a rate of 2 °C/min and an oscillation amplitude of 0.212 °C because 4 modulation cycles at half-height of the melting peak could not be achieved at 3 °C/min.

3. Results

3.1. Copolyester composition and sequence distribution

The assignment of the ^{13}C NMR spectra of the PET/PTT copolyesters is based on the ^{13}C NMR results of PET and

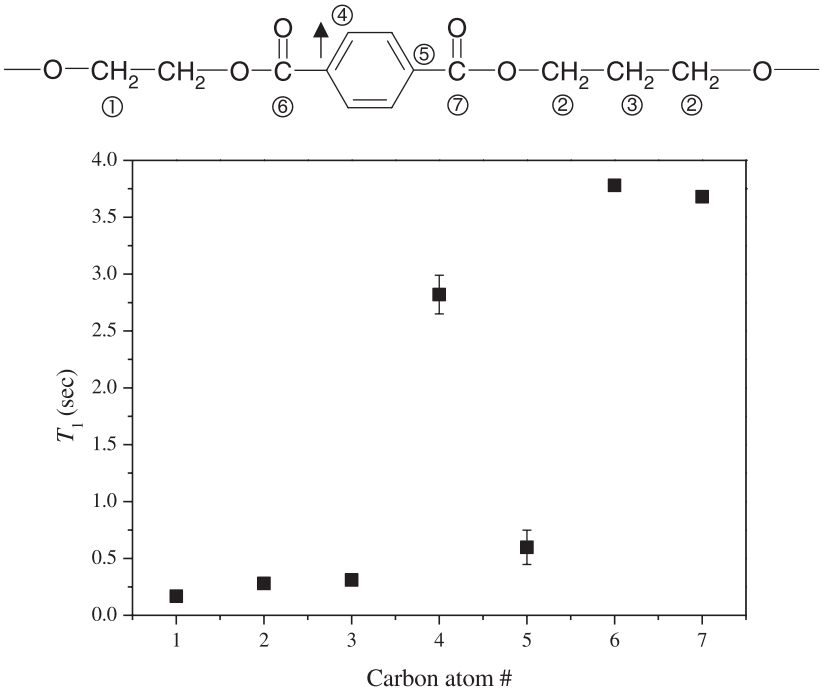

Fig. 1. The spin-lattice relaxation time (T_1) by 100.63 MHz ^{13}C NMR.

PTT homopolymers. The chemical shift of quaternary aromatic carbons is in the range of 133.6–134.0 ppm [16]. A close view of the spectra is plotted in Fig. 2 for all of this series of polyesters. The quaternary aromatic carbons have four peaks in the case of copolyesters. The peak height at 133.7 ppm increases as the content of ET increases from 9 to 91 mol% while the peak height at 133.8 ppm decreases. Moreover, the peak height at 133.6 ppm is close to that at 133.9 ppm. From the chemical shift of PTT homopolymer, 133.8 ppm is assigned to the quaternary aromatic carbons with trimethylene- units on both sides, abbreviated with a symbol of PTP. Similarly, the chemical shifts for ETP-E side, ETE, and ETP-P side (where E represents ethylene glycol unit, T is terephthalate unit, and P denotes 1,3-propanediol unit) are at 133.6, 133.7, and 133.9 ppm, respectively. These four peaks are sufficient to characterize the changes in the chain structure.

The total areas of four peaks in Fig. 2 are normalized to 1 for each copolyester, and their percent values of each peak area are listed in columns 2–5 of Table 2 under the subtitles of ETE, PTP, ETP-E side and ETP-P side. There are three possible triad sequences in the PET/PTT copolyester - ETE, PTP, and ETP. Two peaks of equal intensity are observed for the unequivalent carbons in the mixed diester sequence ETP. Then the probabilities of triads are calculated from the normalized areas, and tabulated in columns 6–8 of the same Table. In the case of PT91/ET09, *P*(ETE), *P*(PTP) and *P*(ETP) are 0, 82.2 and 17.8%, respectively. This copolymer is characterized to have 91.1 mol% PT unit, and 8.9 mol% ET unit, as shown in the second row of Table 3. The

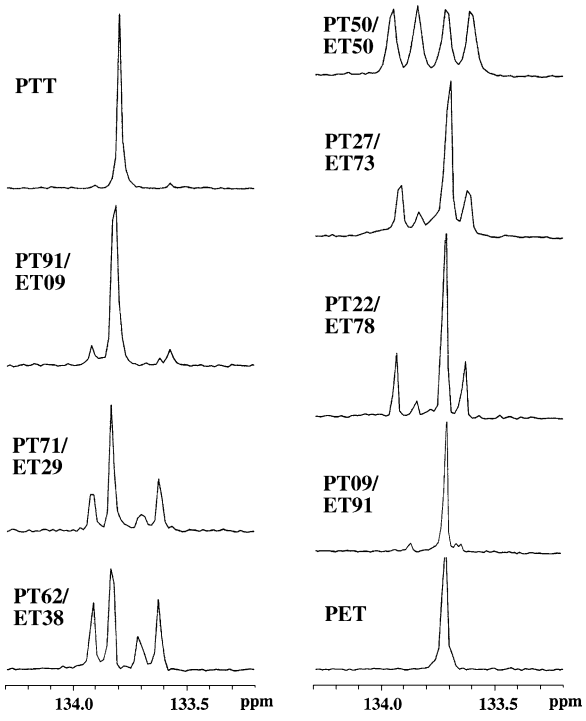

Fig. 2. The quaternary aromatic carbons of PET/PTT copolyesters by ^{13}C NMR.

randomness or irregularity factor *B* [17,18] is given by $P(ETP)/(2P_{PT} \times P_{ET})$, where P_{PT} and P_{ET} are the mole fraction of PT and ET units. The *B* value is 1.10. The average number sequence lengths [17,19] for PT and ET units are 10.2 [$2P_{PT}$ / *P*(ETP), Ln_{PT}] and 1.0 [$2P_{ET}$/*P*(ETP), Ln_{ET}], respectively. It suggests that Ln_{PT} is much longer than Ln_{ET} for this copolyester. This finding suggests the sequence distribution of this copolyester is nearly randomly.

In the case of PT50/ET50 copolyester, four peak areas of the quaternary aromatic carbons are almost equivalent (25.5–23.9%, see the fourth row of Table 2). The components of ET and PT units are in equal amounts, 49.9 and 50.1 mol%, as shown in Table 3. The values of *B*, Ln_{PT} and Ln_{ET} are 0.98, 2.0 and 2.0, respectively. It can be confirmed that ET and PT units are random distributed in this copolymer with average sequence length of 2 ET and 2 PT units. Similarly, Ln_{ET} of PT09/ET91 copolyester is equal to 9.9 and the corresponded Ln_{PT} is 1.0; it suggests that Ln_{ET} is much longer than Ln_{PT} for the copolyester with composition of 9.2 mol% of PT and 90.8 mol% of ET. All of these copolymers in Table 3 have *B* values of about 1.0, therefore, they may be regarded as copolyesters with random distribution.

In this series, of PET/PTT copolyesters, the chemical shifts of ^{1}H NMR in the range of 4.71–4.84 ppm, 4.49–4.64 ppm and 2.29–2.42 ppm represent the ethylene protons in the $–OCH_2CH_2O–$ unit and the methylene protons α and β to the ester oxygen in the $–OCH_2CH_2CH_2O–$ unit, respectively. For comparison, the compositions were also determined from the integration areas of the center methylene proton in the 3G moiety at ~2.3 ppm relative to the methylene proton in the 2G moiety at ~4.8 ppm [10]. The results from the ^{1}H NMR spectra are tabulated in columns 7 and 8 of Table 3, which are within the experimental error of those observed in the ^{13}C NMR spectra.

3.2. Non-isothermal crystallization

Fig. 3A shows the heating thermograms of the amorphous samples from the glass state. In this figure and the following figures, legends (a)–(i) represent PTT, PT91/ET09, PT71/ET29, PT62/ET38, PT50/ET50, PT27/ET73, PT22/ET78, PT09/ET91, and PET, respectively. For all curves of these PET/PTT copolyesters, a clear glass transition temperature (T_g), an exothermic peak of cold crystallization, and an endothermic melting peak are detected. T_g was between 44 °C (for PTT) and 78 °C (for PET), and increased linearly as the composition of the ET unit increased. All of the random copolyesters synthesized in this study are crystallizable and the T_m's of the homopolyester shows at 228 and 253 °C, respectively, for PTT and PET. The T_m's of the copolyesters showed a tendency to decrease to 165 °C at PT50/ET50, a copolyester with equal amounts of PT and ET units. Also, the enthalpy of cold crystallization and the heat of fusion showed a

Table 2
Normalized peak areas of the aromatic quaternary carbons and the triad sequence probabilities by ^{13}C NMR

Sample code	Normalized peak areas of the aromatic quaternary carbons (%)				Triad sequence probabilities (%)		
	ETE	PTP	ETP-E side	ETP-P side	*P*(ETE)	*P*(PTP)	*P*(ETP)
PT91/ET09	0	82.2	8.8	9.0	0	82.2	17.8
PT71/ET29	9.4	50.3	21.2	19.1	9.4	50.3	40.3
PT62/ET38	14.5	38.7	23.6	23.2	14.5	38.7	46.8
PT50/ET50	25.5	25.3	25.3	23.9	25.5	25.3	49.2
PT27/ET73	53.4	8.5	18.7	19.4	53.4	8.5	38.1
PT22/ET78	61.2	5.6	16.7	16.5	61.2	5.6	33.2
PT09/ET91	81.6	0	11.4	7.0	81.6	0	18.4

similar tendency to T_m. The shape of cold crystallization is sharper and narrower for PTT and PT91/ET09, as shown in curves a and b of Fig. 3A. Their peak temperatures of cold crystallization (T_{cc}) are at 66 and 71 °C, respectively, which are only 22 or 26 °C above their T_g. The T_{cc}'s of the copolyesters shifts to 107 and 140 °C as the content of ET increases up to 29 and 50 mol%, and the temperature difference between T_{cc} and T_g becomes significant. The lowest enthalpy of cold crystallization and the highest T_{cc} for PT50/ET50 result in a small and broad peak of cold crystallization. The corresponding melting peak of PT50/ET50 is also the smallest among these polyesters. On the other hand, the T_{cc}'s of the copolyesters with ET mol% $\geq$73 is between 119 and 135 °C. Their shape of cold crystallization is similar. There is no tendency of shifting T_{cc} to higher temperature with increasing ET. As can be seen in the cooling thermograms of Fig. 3B, the shape of melt crystallization peak is also sharp and narrow for PTT and PT91/ET09. The shape for PET is broader although its melt crystallization starts 15 °C higher than PTT does. The peak and the peak temperature gradually become broader and lower as the content of minor co-monomer increases. Finally, the peak of melt crystallization disappears completely in the cases of PT50/ET50 and PT27/ET73.

3.3. Wide angle X-ray diffraction

WAXD patterns for PTT, PET, and PET/PTT copolyesters are shown in Fig. 4. The crystal unit cell of PTT is triclinic and diffraction peaks from (010), (0$\bar{1}$2), (012), (100), (102, 10$\bar{3}$), and (1$\bar{1}$3) are observed at $2\theta \approx 15.6$, 17.2, 19.5, 21.8, 23.7, and 24.9°, respectively [20–25]. The diffraction patterns of triclinic PET at 2θ value of $\approx$16.3, 16.8, 21.8, 22.9, 26.2, and 28.1°, corresponding to the reflection planes of (0$\bar{1}$1), (010), ($\bar{1}$11), ($\bar{1}$10), (100), and (1$\bar{1}$1), respectively [26]. The WAXD patterns are divided into three groups according to the PT content in the copolyester. PT91/ET09 and PT71/ET29 copolyesters show the WAXD patterns as that of PTT (see curves a–c), and the intensity of diffraction peaks decreases with increasing content of ET moieties. PET triclinic crystals mainly develop above 73 mol% ET content as shown in curves f-i of Fig. 4, and the intensity of diffraction peaks decreases with increasing content of PT moieties. As a consequence of comonomer inclusion, the *d* spacings of both crystal structures change with the comonomer content. In the PTT type, both the *d*(100) and the *d*(010) spacings slightly decrease with increasing ET content. However, in the case of PET type crystal, both the *d*(100) and the *d*(010) spacings are almost constant irrespective of the PT content. On the other hand, the WAXD pattern of PT50/ET50 is quite different from those of PET and PTT, and that of PT62/ET38 shows the mixed diffraction peaks of PT71/ET29 and PT50/ET50.

In addition, it was found that there was no positional change of the diffraction peaks through the WAXD measurement [27] for the individual polyester crystallized at various temperatures isothermally (T_c). Fig. 5 shows the

Table 3
Sample codes, the composition calculated from both ^{13}C and ^{1}H NMR spectra, the randomness parameter (*B*), and the average-number sequence lengths of PT and ET units

Sample code	From ^{13}C NMR					From ^{1}H NMR	
	PT(%)	ET(%)	*B*	Ln_{PT}	Ln_{ET}	PT(%)	ET(%)
PTT	100	0				100	0
PT91/ET09	91.1	8.9	1.10	10.2	1.0	93.1	6.9
PT71/ET29	70.5	29.5	0.97	3.5	1.5	71.7	28.3
PT62/ET38	62.1	37.9	0.99	2.7	1.6	62.3	37.7
PT50/ET50	49.9	50.1	0.98	2.0	2.0	50.8	49.2
PT27/ET73	27.5	72.5	0.96	1.4	3.8	27.2	72.8
PT22/ET78	22.2	77.8	0.96	1.3	4.7	23.4	76.6
PT09/ET91	9.2	90.8	1.10	1.0	9.9	10.2	89.8
PET	0	100				0	100

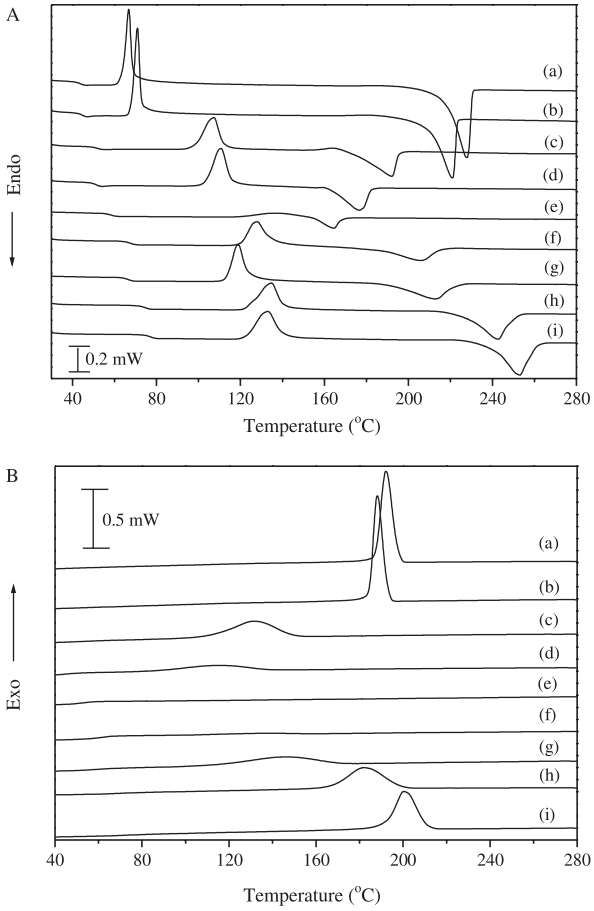

Fig. 3. Non-isothermal DSC thermograms at heating (A) and cooling (B) rates of 5 °C/min for melt-quenched homo- and co-polyesters of: (a) PTT, (b) PT91/ET09, (c) PT71/ET29, (d) PT62/ET38, (e) PT50/ET50, (f) PT27/ET73, (g) PT22/ET78, (h) PT09/ET91, (i) PET.

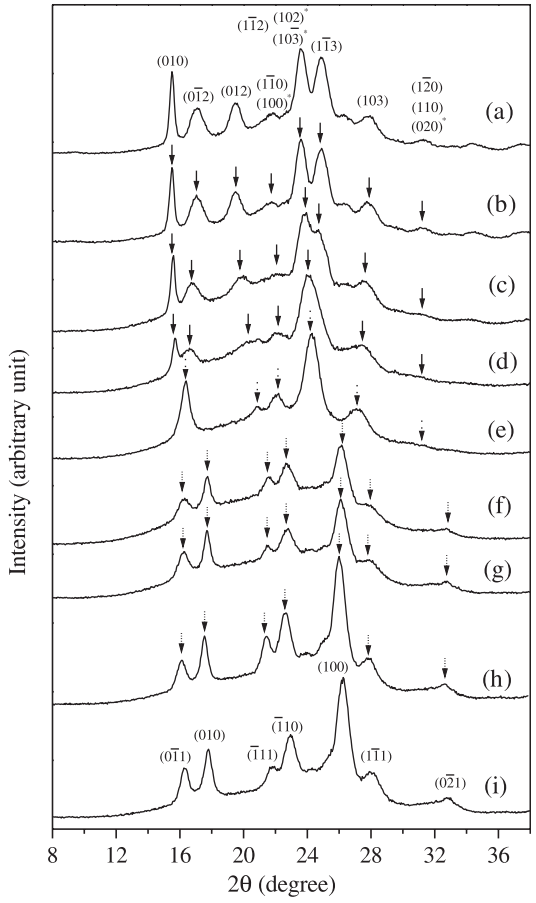

Fig. 4. X-ray diffraction patterns for isothermally melt-crystallized copolyesters of: (a–i) see caption of Fig. 3. The asterisk (*) indicates the major reflection in the diffraction peak.

WAXD example patterns of PT91/ET09 copolyester melt-crystallized isothermally at various T_c ranging from 183 to 207 °C in an interval of 6 °C. The pattern of diffraction peaks, the value of 2θ for each diffraction peak and crystal cell parameters are the same as each other, suggesting that the crystal structure of this copolyester is a triclinic system in the same manner as is PTT. It is obvious that each copolyester has its characteristic diffraction peaks. These peaks become stronger as T_c increases. The results indicate that there is only one crystal structure regardless of T_c for the individual polyester.

3.4. Melting behavior after non-isothermal cooling

Like crystallizable polymers, non-isothermal DSC cooling thermogram of the PET/PTT copolyester shows a typical single crystallization exotherm, similar to Fig. 3B. The characteristic data of non-isothermal crystallization are tabulated in columns 4–7 of Table 4, including the onset temperature (T_{onset}), the peak temperature (T_p), the end temperature (T_{end}), and the enthalpy (ΔH_c) of crystallization, respectively. It is found that the values of T_{onset}, T_p, T_{end}, and ΔH_c decrease as the content of minor co-monomer increases. The first row of Table 4 shows that the PT91/ET09 sample starts to crystallize at 195.8 °C, and reaches a maximum at 186.0 °C. The detectable signal of non-isothermal crystallization of PT91/ET09 disappears at

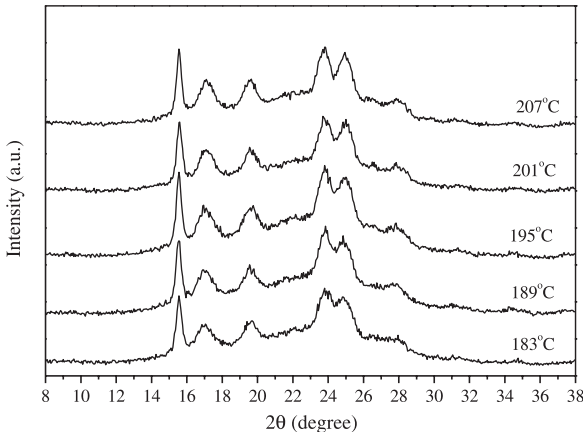

Fig. 5. WAXD powder patterns of PT91/ET09 copolyester after the samples were completely crystallized isothermally at the indicated temperature ranging from 183–207 °C.

Table 4
Data of non-isothermal crystallization and thermal properties of poly(ethylene terepathalate-*co*-trimethylene terepathalate)s

Sample code	T_m^0 (HW)[a] (°C)	T_{molten} (°C)	T_{onset} (°C)	T_p (°C)	T_{end} (°C)	ΔH_c (J/g)	$T_{II\rightarrow III}$ (°C)	$T_{I\rightarrow II}$ (°C)
PT91/ET09	237	252	195.8	186.0	173.5	48.3	193.6	210–213
PT71/ET29	197	215	157.3	125.3	93.4	34.0	147.3	170–174
PT62/ET38	188	192	142.0	117.2	75.4	13.0	140.4	164–168
PT27/ET73	227	228	169.3	155.7	127.1	26.9	164.8	
PT22/ET78	230	234	186.0	169.3	133.0	30.2	172.0	
PT09/ET91	261	276	206.8	173.6	126.2	38.7	208.4	228–232

T_{molten}: the pre-melting temperature before the non-isothermal crystallization. T_{onset}: the onset temperature, T_p: the peak temperature, T_{end}: the end temperature, and ΔH_c: the enthalpy of crystallization. $T_{II\rightarrow III}$: Transition temperature of regime II → III [16,33,64]. $T_{I\rightarrow II}$: Transition temperature range of regime I → II [27].
[a] Hoffman-Weeks plot from the primary melting peak measured at a rate of 50 °C/min [33].

~173.5 °C, and its enthalpy of melt crystallization, 48.3 J/g, is the highest one among these copolyesters. The ΔH_c of PT62/ET38 is 13.0 J/g, which is the smallest one. The ΔH_c of the rest of the four copolyesters ranges from 26.9 to 38.7 J/g.

Fig. 6 show the total heat flow curves of TMDSC for six copolyesters. In the case of PT91/ET09 at a heating rate of 2 °C/min (curve b), two sharp melting peaks merge together with peak temperatures at 218 and 223 °C, and a small exothermic peak at 209 °C appears just prior the melting. Single melting peak at 193 °C (curve c) is seen for the PT71/ET29 sample, leading with a small melting and recrystallization curves at a heating rate of 3 °C/min. Curve d shows a broad cold crystallization peak ranging from 80 to 125 °C with peak temperature at 110 °C, and a single melting peak at 178 °C for the PT62/ET38 sample. However, the exothermic recrystallization is not detected in this curve and curves f, g and h. In comparison, the PT27/ET73 and PT22/ET78 samples reveal a small melting curve with a long leading head, followed by two broad melting peaks that overlap together, as shown in curves f and g. The PT09/ET91 sample has a single melting peak at 242 °C, leading with a small and long melting curve (see curve h).

Fig. 7 shows the triple melting peaks with a leading head in the reversing curves of TMDSC for the PT91/ET09, PT71/ET29, and PT62/ET38 samples. The middle peak is the strongest one, as shown in curves b, c, and d. The PT91/ET09 sample starts to melt at about 164 °C and extends up to 228 °C with peak temperatures at 206, 218, and 223 °C. The apparent peak temperatures are 177, 187, and 194 °C for PT71/ET29, and are 159, 171, 182 °C for PT62/ET38, respectively. Curves f and g present a single broad melting peak with a small, long leading head in the low temperature side, and a small shoulder in the high temperature side for the PT27/ET73 and PT22/ET78 samples. A very broad melting curve, with a long leading head starting at 152 °C, is observed in curve h for the PT09/ET91 sample.

In the non-reversing thermograms of TMDSC (see Fig. 8), a strong exothermic recrystallization can be found in curves b, c, d and h, but a small and broad exothermic signal is seen in curves f and g. In the case of PT91/ET09 at a heating rate of 2 °C/min (curve b), the exothermic process starts from ~184 °C, increases slowly at the beginning, reaches a distinct sharp peak at 207 °C, and finally extends up to 215 °C, which is immediately followed with a sharp melting peak at 223 °C. In comparison, the PT71/ET29 sample at a heating rate of 3 °C/min reveals a broad recrystallization process, which starts from about 140 °C and extends up to 184 °C, as shown in curve c. The PT62/ET38 sample at a heating rate of 3 °C/min is plotted in curve d, which presents both exothermic processes of cold

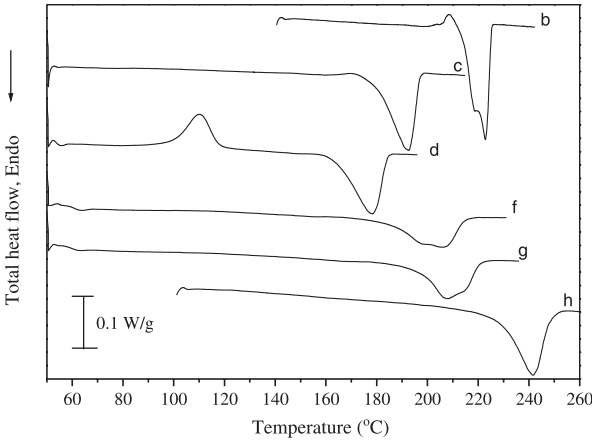

Fig. 6. Total heat flow of TMDSC thermograms for the copolyesters after non-isothermal crystallization: (b–h) see caption of Fig. 3.

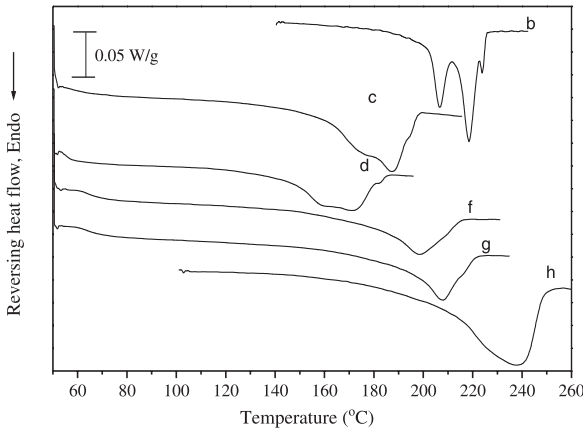

Fig. 7. Reversing heat flow of TMDSC thermograms for the copolyesters after non-isothermal crystallization: (b–h) see caption of Fig. 3.

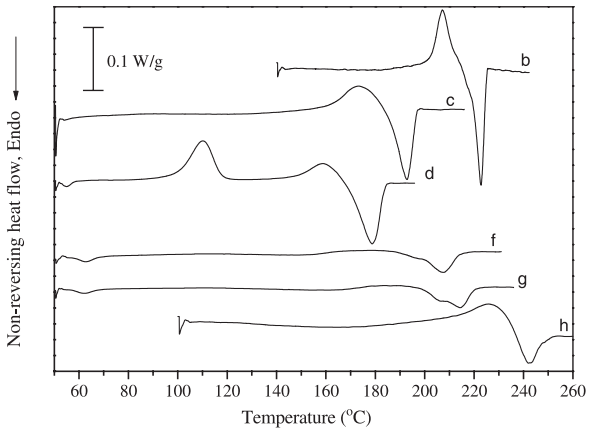

Fig. 8. Non-reversing heat flow of TMDSC thermograms for the copolyesters after non-isothermal crystallization: (b–h) see caption of Fig. 3.

crystallization and recrystallization. The cold crystallization starts from ~77 °C, and the recrystallization ends apparently at 168 °C. Small exothermic curves can be seen between these two exothermic peaks. In the case of PT09/ET91, the exothermic process starts from ~160 °C, increases slowly, and leads to a broad peak which ends apparently at 237 °C.

4. Discussion

4.1. Random copolyesters

Tables 1 and 3 show that the content of 3G (or PT unit) incorporated into the copolyester is always larger than that fed in the bulk polymerization. This result might come mainly from three reasons as follows. First, 3G has a relatively high boiling point (214 °C) than that of 2G (197 °C). Thus, 3G is less volatile than 2G, so that 2G component is removed more easily than 3G in the polycondensation, leading to a high content of 3G unit in the resultant copolymer [13]. Second, oligomer of BHPT was produced before the esterification with terephthalic acid and 2G in this study. Third, the rate constants of copolycondensation between BHPT and bis(2-hydroxyethyl) terephthalate (BHET) is in favor of BHPT in the early reaction stage [28].

In Fig. 3A, PET polymer exhibits T_g at 78 °C while the PTT polymer reveals T_g at 44 °C. The copolyesters have intermediate T_g between those of the parent homopolyesters. That is, T_g in the copolyester is depressed with increasing the content of 3G unit. Such T_g depression is attributed to the chain flexibility enhanced by the incorporation of 3G unit. Further, all of the copolymers exhibit a single T_g rather than two T_g's corresponded to possible blocks of PET and PTT. In addition, all of these copolyesters have B (randomness parameter) values of about 1.0, which is obtained from the ^{13}C NMR analysis (see Table 3). These results have demonstrated that comonomer placement in these copolymers is essentially random.

4.2. Crystallizability

PET and PTT are semicrystalline polymers. The incorporation of co-monomeric units into the polymer backbone leads to an irregular chain structure and thereby inhibits regular chain packing for crystallization. The crystallization of PET/PTT copolyesters is strongly influenced by the chain microstructure regarding co-monomer distribution, randomness and length of the crystallizable ET or PT sequences. The random distribution of ET and PT units is discussed in the previous section, and the average number sequence lengths of ET and PT units are listed in Table 3. Generally, as the ratio of two components of copolymer increases, the WAXD pattern is affected by the predominant crystal unit, as shown in Fig. 4. Therefore, the WAXD patterns of PT91/ET09 and PT71/ET29 are influenced by the diffraction pattern of the PTT unit. Also, in the WAXD patterns of PT27/ET73, PT22/ET78 and PT09/ET91, the diffraction pattern of the PET unit is dominant. In the copolyesters of PT91/ET09 and PT09/ET91, L_n of the major component is ~10 and L_n of the minor one is 1.0 only. It can therefore be presumed that the segments containing minor co-monomer moieties less than 10 mol% in the copolymer are not in the crystal unit cell of the copolymer but in the amorphous phase between the crystalline lamellae according to the exclusion crystallization model of Flory [29–32].

As mentioned in Section 4.1, the content of 3G incorporated into the copolyester is always larger than that fed. There is no copolyester with composition of 27 mol% < 3G < 50 mol% in this study. By means of isothermal [33–35] and non-isothermal [27] DSC experiments, it was found that all of the random copolyesters used in this study are crystallizable. The WAXD patterns in Fig. 4 also prove that the PET/PTT copolyesters containing 71, 60 or 50 mol% of 3G are crystallizable. This result is different from that reported by Smith et al. [9], Ponnusamy, Balakrishnan [10,11], and Wu, Lin [14]. It might come from the low molecular weight [10,11] and the pre-melting conditions. If the pre-melting temperature is too high above T_m^0 and/or the pre-melting time is too long, the nucleation rate will decrease significantly. In addition, if the growth rate is slow, too, the crystallization will not be detected. Some of the measured non-isothermal DSC thermal analysis curves are shown in Fig. 3 with a pre-melting condition of 285 °C, 3 min for all the polyesters. The homopolyesters show relatively narrower exothermic peaks than those of their copolyesters. The enthalpies of cold-crystallization, fusion and melt-crystallization decreased as the content of minor co-monomer increased. Therefore, the non-isothermal crystallization was not detected for PT50/ET50 and PT27/ET73 copolyesters (see curves e and f in Fig. 3B). The

same reason can explain the amorphous behavior of the copolyester with 56.5 mol% 3G [14] because the pre-melting condition of 40 °C above T_m and 20 min was too high and too long for the copolyesters with close contents of ET and PT.

The change of melting temperatures with the ET compositions reveals a typical eutectic behavior (see Fig. 3A). The minimum melting temperature is observed at 165 °C for PT50/ET50, a random copolyester with average sequence length of 2.0 for both ET and PT units. If the exclusion crystallization model is applied to the PT50/ET50 crystal, the maximum lamellar thickness (or the length of crystallizable sequences) will be only 21.6 or 18.6 Å based on the c-axis value of PET [36] and PTT [20–25]. The study on the crystallization process of the PT50/ET50 sample by real-time in situ SAXS is currently underway and will be reported in a separate manuscript. From the DSC results of isothermal crystallization between 115 and 142 °C [34,35], the PT50/ET50 copolymer had heat of fusion ranging from 30.2 to 36.7 J/g. These values are about 25% absolute crystallinity based on the heat of fusion, 122 J/g and 146 J/g, for 100% crystalline PET [37] and PTT [38], respectively. The reason for such copolyester being able to co-crystallize could be due to the similar chemical structure of 3G and 2G. Increasing the minor co-monomer content, the crystallization rates of the copolymers decrease, that is due to the lower rates of nucleation and crystal growth [33–35].

4.3. Multiple melting behavior

DSC heating scans, after isothermal or non-isothermal crystallization, showed multiple melting endotherms for aromatic polyesters and copolyesters [13,16,33–35,39–51]. Traditional DSC measurements result from the summation of endothermic and exothermic processes. They are often confusing and sometimes misleading, thus no further information can be used to explain the melting behavior, especially when multiple transitions (e.g. crystallization, melting) appear in the same temperature range. TMDSC [52–63] provides not only a total heat flow (like traditional DSC) but also the reversing and the non-reversing heat flow. Therefore, TMDSC was used in this work to characterize the melting and recrystallization behavior of the PET/PTT copolyesters after non-isothermal crystallization. Before proposing a model to explain the complex melting behavior of the PET/PTT copolyesters, it must be pointed out that the crystal form of PET/PTT did not change with the temperature. Based on the WAXD patterns of Fig. 5 for PT92/ET08, there is only one crystal structure formed in this temperature range. The possibility of different crystal structures is excluded for this copolyester. Therefore, the multiple melting peaks may be due to the melting of two populations of lamellar crystals and/or the melting-recrystallization-remelting processes.

Comparing the peak temperature of non-isothermal crystallization (see T_p in Table 4) to the temperature at the lowest temperature peak in the reversing curve (see Fig. 7), it can be observed that in all cases the data from the melting is at least 20 °C higher than those from the crystallization. It can also be observed that the recrystallization starts immediately after melting of the crystals at lower temperature by comparing the starting temperature of the melting endotherm observed in the reversing curves with the starting temperature of the exothermic signal observed in the nonreversible curves (see Fig. 8), except one more crystallization peak is detected in curve d. In the case of PT62/ET38, the original crystallinity ($\Delta H_c = 13.0$ J/g, see Table 4) resulting from the non-isothermal crystallization is low. Cold crystallization can be detected in both of the total and non-reversing heat flows (see curve d of Figs. 6 and 8) because the time is not long enough to complete the non-isothermal crystallization of the PT62/ET38 sample at a cooling rate of 5 °C/min. In addition, the peak temperature of major melting endotherms appears at 10–15 °C above the peak temperature of the exothermic peak. For the PET/PTT copolyesters crystallized non-isothermally from the melt at a constant cooling rate of 5 °C/min, all the facts mentioned above confirmed that the multiple melting behavior originates in the melting and recrystallization of the crystallites of the low melting endotherm with low thermal stability. The higher melting endotherms correspond to the melting of the crystallites with high thermal stability formed through the recrystallization of the melt of the crystallites of the low melting endotherms. Recrystallization can more rapidly produce crystalline material than ordinary isothermal crystallization at the same temperature because the kinetics is enhanced by the presence of unmolten nuclei. For the PT27/ET73 and PT22/ET78 copolyesters, the non-reversing curves showed that the exothermic signal was small and broad suggesting that during the TMDSC heating scan very little recrystallization was observed. These results indicated that the nucleation rate and growth rate were reduced significantly by incorporating the PT unit into the PET chain. Therefore, part of the double melting peaks in curves f and g of Fig. 6 is due to the melting of two populations of lamellar crystals. The experimental results suggest that the melting behavior of PET/PTT copolyesters in this study is most convincingly explained on the basis of the melting-recrystallization-remelting model.

In the reversing curve, there are three distinct peaks of melting in the case of PT91/ET09. Three broad and overlapping peaks are also observed in the reversing melting curves of PT71/ET29 and PT62/ET38, as shown in Fig. 7. It is noted that one additional minor endotherm located in the high temperature side. One additional endotherm was also reported by Wu and Lin [14] for PTT and PET/PTT copolyester containing 91.4 mol% PT using conventional DSC. This phenomenon was observed only when these two polyesters were crystallized at lower T_c's and it was explained as the fusion of recrystallized crystallites with different stabilities. In this study, two

peaks in the high temperature side are also due to remelting of the recrystallized crystals formed during the heating scan (see Fig. 8), whereas the highest one is attributed to the melting of the crystals that are formed in relatively high temperature or in regime I [27]. The transition temperatures of regime II→III and I→II are listed in the last two columns of Table 4 as a reference [16,27,33,64]. The manuscripts of regime study are currently in preparation and will be submitted soon.

5. Conclusion

A series of PET/PTT copolyesters were synthesized in a random sequence, which was supported from the evidence of a single T_g and a randomness value of ~1.0. The results of WAXD patterns and non-isothermal DSC thermograms from the amorphous glass state provide a direct evidence to support the crystallization behavior of all these copolyesters synthesized in this study. The WAXD pattern is either PTT triclinic or PET triclinic depending on the predominant monomer unit. The PT50/ET50 copolyester is still crystallizable even though the average sequence length is only 2.0 for both ET and PT units, and its WAXD pattern is quite different from those of PET and PTT homopolyesters. Based on the results of WAXD and TMDSC, the existence of two melting mechanisms, i.e. the recrystallization process and dual morphologies, becomes evident. It is suggested that the melting behavior of PET/PTT copolyesters in this study is most convincingly explained on the basis of the melting-recrystallization-remelting model.

Acknowledgements

The authors acknowledge the financial support of the National Science Council of Taiwan, ROC, through Grants NSC 90-2216-E-110-014 and 92-2216-E-110-011.

References

[1] Whinfield JR, Dickson JT. Brit. Patent 578,079, June 14; 1946.
[2] Whinfield JR, Dickson JT. US Patent 2,465,319, March 22; 1949.
[3] Goodman I. Polyesters. In: Kroschwitz JI, editor. Encyclopedia of polymer science and engineering, 2nd ed, vol. 12. New York: Wiley; 1988. p. 10.
[4] Brown HS, Chuah HH. Chem Fiber Int 1997;47:72.
[5] Wunderlich B. Macromolecular physics. vol. 2. New York: Academic Press; 1976.
[6] Jog JP. J Macromol Sci Rev Macromol Chem Phys 1995;C35:531.
[7] Chen CC, Chen M, Tseng IM. J Macromol Sci Phys 2002;B41:1043.
[8] Chen M, Chen CC, Ke KZ, Ho RM. J Macromol Sci Phys 2002;B41: 1063.
[9] Smith JG, Kibler CJ, Sublett BJ. J Polym Sci Part A-1: Polym Chem 1966;4:1851.
[10] Ponnusamy E, Balakrishnan T. J Macromol Sci Chem 1985;A22:373.
[11] Ponnusamy E, Balakrishnan T. Polym J 1985;17:473.
[12] Kiyotsukuri T, Masuda T, Tsutsumi N. Polymer 1994;35:1274.
[13] Lee JW, Lee SW, Lee B, Ree M. Macromol Chem Phys 2001;202: 3072.
[14] Wu TM, Lin YW. J Polym Sci Part B: Polym Phys 2004;42:4255.
[15] TA Instruments. DSC 2910 differential scanning calorimeter, Operator's manual, Rev.8. New Castle, Delaware; 1997. p. C-73.
[16] Chen M, Wang HC, Ko CY. Abstr Pap Am Chem 2002;S 224. 166-POLY Part 2 Aug 18.
[17] Newmark RA. J Polym Sci, Polym Chem Ed 1980;18:559.
[18] Yamadera R, Murano M. J Polym Sci A-1 Polym Chem 1967;5:2259.
[19] Backson SCE, Kenwright AM, Richards RW. Polymer 1995;36:1991.
[20] Ho RM, Ke KZ, Chen M. Macromolecules 2000;33:7529.
[21] Wang B, Li CY, Hanzlicek J, Cheng SZD, Geil PH, Grebowicz J, Ho RM. Polymer 2001;42:7171.
[22] Srimoaon P, Dangseeyun N, Supaphol P. Eur Polym J 2004;40:599.
[23] Poulin-Dandurand S, Pérez S, Revol JF, Brisse F. Polymer 1979;20: 419.
[24] Moss B, Dorset DL. J Polym Sci Polym Phys Ed 1982;20:1789.
[25] Dorset DL, Moss B. Polymer characterization. Washington, DC: American Chemical Society; 1983. Chapter 22.
[26] Daubeny RP, Bunn CW, Brown CJ. Proc R Soc London Ser A 1954; 226:531.
[27] Ko CY. Master Thesis, National Sun Yat-sen University, Kaohsiung, Taiwan; 2003.
[28] Kim JH, Lee SY, Park JH, Lyoo WS, Noh SK. J Appl Polym Sci 2000; 77:693.
[29] Flory PJ. J Chem Phys 1947;15:684.
[30] Flory PJ. J Chem Phys 1949;17:223.
[31] Flory PJ. Trans Faraday Soc 1955;51:848.
[32] Baur VH. Makromol Chem 1966;98:297.
[33] Wang HC. Master Thesis, National Sun Yat-sen University, Kaohsiung, Taiwan; 2002.
[34] Chang CW. Master Thesis, National Sun Yat-sen University, Kaohsiung, Taiwan, 2004.
[35] Chang CW, Ko CY, Chen M. Program & Abstracts of the 27th ROC. Polymer Symposium in Tamsui, Taipei County, Taiwan, February 21–22; 2004, p. 216.
[36] Holdsworth PJ, Turner-Jones A. Polymer 1971;12:195.
[37] Roberts RC. Polymer 1969;10:113.
[38] Pyda M, Boller A, Grebowicz J, Chuah H, Lebedev BV, Wunderlich B. J Polym Sci Part B: Polym Phys 1998;36:2499.
[39] Groeninckx G, Reynaers H, Berghmans H, Smets G. J Polym Sci Polym Phys Ed 1980;18:1311.
[40] Zhou C, Clough SB. Polym Eng Sci 1988;28:65.
[41] Medellín-Rodríguez FJ, Phillips PJ. Macromolecules 1996;29:7491.
[42] Liu J, Geil PH. J Macromol Sci Phys 1997;36:61.
[43] Qiu G, Tang ZL, Huang NX, Gerking L. J Appl Polym Sci 1998;69: 729.
[44] Wang ZG, Hsiao BS, Sauer BB, Kampert WG. Polymer 1999;40: 4615.
[45] Lu XF, Hay JN. Polymer 2001;42:9423.
[46] Kong Y, Hay JN. Polymer 2003;44:623.
[47] Chung WT, Yeh WJ, Hong PD. J Appl Polym Sci 2002;83:2426.
[48] Wu PL, Woo EM. J Polym Sci Part B: Polym Phys 2002;40:1571.
[49] Huang TW, Chen M. Program and Abstracts of PPS-2002 Asia/Australia Meeting in Taipei, Taiwan, November 4–8; 2002, p. 118.
[50] Wu PL, Woo EM. J Polym Sci Part B: Polym Phys 2003;41:80.
[51] Srimoaon P, Dangseeyun N, Supaphol P. Eur Polym J 2004;40:599.
[52] Reading M. Trends Polym Sci 1993;8:248.
[53] Reading M, Elliott D, Hill VL. J Therm Anal 1993;40:949.
[54] Reading M, Luget A, Wilson R. Thermochim Acta 1994;238:295.
[55] Okazaki I, Wunderlich B. Macromol Rapid Commun 1997;18:313.
[56] Okazaki I, Wunderlich B. Macromocules 1997;30:1758.
[57] Wurm A, Merzlyakov M, Schick C. Colloid Polym Sci 1998;276:289.
[58] Wurm A, Merzlyakov M, Schick C. J Macromol Sci Phys 1999;B38: 693.

[59] Sauer BB, Kampert WG, Neal Blanchard E, Threefoot SA, Hsiao BS. Polymer 2000;41:1099.
[60] Kampert WG, Sauer BB. Polym Eng Sci 2001;41:1714.
[61] Kampert WG, Sauer BB. Polymer 2001;42:8703.
[62] Wunderlich B. Prog Polym Sci 2003;28:383.
[63] Wei CL, Chen M, Yu FE. Polymer 2003;44:8185.
[64] Wang HC, Chen RY, Wang CL, Ko CY, Chen M. Program & Abstracts of PPS-2002 Asia/Australia Meeting in Taipei, Taiwan, November 4–8; 2002, p. 119.